DOI:10.1021/jf903068k

JOURNAL OF AGRICULTURAL AND FOOD CHEMISTRY
ARTICLE

Polyphenols from *Broussonetia papyrifera* Displaying Potent α-Glucosidase Inhibition

Hyung Won Ryu,[†] Byong Won Lee,[†] Marcus J. Curtis-Long,[‡] Sunin Jung,[†] Young Bae Ryu,[§] Woo Song Lee,[§] and Ki Hun Park*,[†]

[†]Division of Applied Life Science (BK21 Program), EB-NCRC, Institute of Agriculture and Life Science, Graduate School of Gyeongsang National University, Jinju 660-701, South Korea, [‡]12 New Road, Nafferton, Driffield, East Yorkshire YO25 4JP, United Kingdom, and [§]Molecular Bioprocess Research Center, KRIBB, Jeoungeup 580-185, South Korea

The organic extract of the roots of *Broussonetia papyrifera* showed extremely high α-glucosidase inhibitory activity with an IC_{50} of around 10 μg/mL. Due to its potency, subsequent bioactivity-guided fractionation of the chloroform extract led to 12 polyphenols, **1**−**12**, 4 of which were identified as chalcones (**1**−**4**), another 4 as flavans (**5**−**8**), 2 as flavonols (**9** and **10**), and 2 others as the novel species benzofluorenones (**11** and **12**). Broussofluorenone A (**11**) and broussofluorenone B (**12**) emerged as new compounds possessing the very rare 5,11-dioxabenzo[*b*]fluoren-10-one skeleton. These compounds (**1**−**12**) were evaluated for α-glucosidase inhibitory activity to identify their inhibitory potencies and kinetic behavior. The most potent inhibitor, **10** (IC_{50} = 2.1 μM, K_i = 2.3 μM), has an inhibitory activity slightly higher than that of the potent α-glucosidase inhibitor deoxynojirimycin (IC_{50} = 3.5 μM). The novel α-glucosidase inhibitors **11** (IC_{50} = 27.6 μM) and **12** (IC_{50} = 33.3 μM) are similar in activity to sugar-derived α-glucosidase inhibitors such as voglibose (IC_{50} = 23.4 μM). Interestingly, major constituents (**1**, **2**, **6**, **7**, **9**, and **10**) of *B. papyrifera* displayed significant inhibitory activity with IC_{50} values of 5.3, 11.1, 12.0, 26.3, 3.6, and 2.1 μM, respectively. In kinetic studies, chalcones (**1**−**4**) exhibited noncompetitive inhibition characteristics, whereas the others (**5**−**12**) showed mixed behavior.

KEYWORDS: Glycosidase; α-glucosidase inhibitor; flavonoid; *Broussonetia papyrifera*

INTRODUCTION

Broussonetia papyrifera Vent. is renowned as a polyphenol-rich plant, which belongs to the family Moraceae and is distributed throughout China, Korea, and Japan. Its branches, leaves, and roots have been used as a diuretic, tonic, and suppressant for edema in Chinese folk medicine (*1*). Since the first report of the use of broussonin A as a source of phytoalexins by K. Takahashi (*2*), many researchers have focused their energies on the isolation of bioactive polyphenols from *B. papyrifera*. These efforts have demonstrated that its main bioactive constituents are flavans, chalcones, and flavanols. Each set of compounds isolated from this plant has been found to manifest significant biological effects, for example, kazinol B (a flavan) stimulated superoxide anion generation in rat neutrophils (*3*), broussochalcone A (a chalcone) suppressed cytosolic protein kinase (*4*), and a range of flavonols were shown to inhibit the enzyme PTP1B (*5*). Recently, some compounds isolated from this plant, including broussoflavonol F, showed inhibitory activities against mushroom tyrosinase (*6*). However, to the best of our knowledge, there has been no report of the roots of *B. papyrifera* eliciting glycosidase inhibitory activity. Glucosidase inhibition is applicable to the treatment of numerous diseases including diabetes mellitus type 2 (*7*), cancer (*8*), and HIV (*9*). This wide range of uses for glucosidase inhibitors exemplifies the pervasive importance of glycosylation/deconjugation of sugars in such varied processes as cell signaling/recognition, cell cycle regulation, and metabolism. A key enzyme class in these processes is the α-glucosidases (EC 3.2.1.20; α-D-glucoside glucohydrolase), which are a group of exoacting enzymes that play essential roles in carbohydrate metabolism and in glycoprotein processing and quality control. Although members of this class of enzymes share the ability to release a terminal glucose moiety from the nonreducing end of their substrates, they display significant diversity in amino acid sequence and aglycon specificity (*10*). Glycosidases are involved in the biosynthesis and processing of the oligosaccharide chains of N-linked glycoproteins in the endoplasmic reticulum (ER) (*11*). Inhibition of these glycosidases, especially α-glucosidases, has a profound effect on glycan structure, which consequently affects the maturation, transport, secretion, and function of glycoproteins and thus has the power to alter cell−cell or cell−virus recognition processes (*12*−*14*). In addition, by retarding the cleavage of complex carbohydrates, postprandial glucose absorption in vivo can be attenuated, thus regulating blood sugar levels.

*Author to whom correspondence should be addressed (telephone +82-55-751-5472; fax +82-55-757-0178; e-mail khpark@gsnu.ac.kr).

 Published on Web 12/02/2009

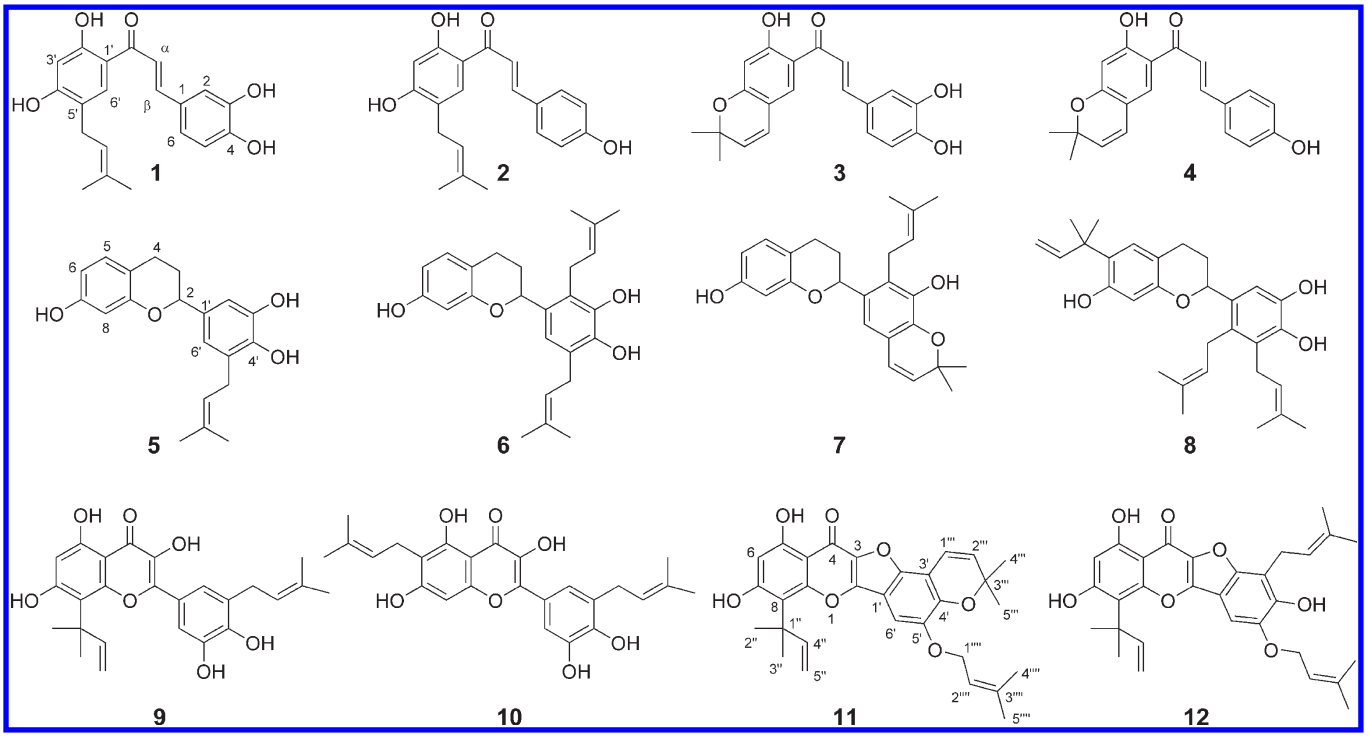

Figure 1. Structures of compounds **1**−**12** isolated from *Broussonetia papyrifera*.

The aim of the present work is to investigate the α-glucosidase inhibitory activities of *B. papyrifera* extracts. We isolated 12 α-glucosidase inhibitory polyphenols together with 2 new compounds that have a very rare 5,11-dioxabenzo[*b*]fluoren-10-one skeleton. All isolated compounds were examined for their α-glucosidase inhibitory activities, and their inhibition mechanisms were ascertained using Lineweaver−Burk and Dixon plots (**Figure 1**).

MATERIALS AND METHODS

Plant Material. The roots of *B. papyrifera* were collected at Gonyang in Sacheon, South Korea, in July 2008 and identified by Prof. Myong Gi Chung. A voucher specimen (KHPark 210709) of this raw material is deposited at the Herbarium of Gyeongsang National University (GNUC).

General Apparatus and Chemicals. Optical rotations were measured on a Perkin-Elmer 343 polarimeter. Melting points were measured on a Thomas Scientific capillary apparatus. UV spectra were measured on a Beckman DU650 spectrophotometer. Infrared (IR) spectra were recorded on a Bruker IFS66 infrared Fourier transform spectrophotometer (on KBr disks). NMR spectra were recorded on a Bruker AM 500 spectrometer with TMS as an internal standard, and chemical shifts are expressed in δ values. Electron impact mass spectrometry (EIMS) measurements were carried out on a JEOL LMS-700 spectrometer. All purifications were monitored by Merck precoated TLC using commercially available glass-backed plates and visualized under UV at 254 and 366 nm or stained with 10% H_2SO_4 solution. Kieselgel 60 silica gel (230−400 mesh) and reversed-phase C18 (RP 18) silica gel (25−40 μm) were used for column chromatography. All solvents used for extraction and isolation were of analytical grade.

Extraction and Isolation. The root bark of *B. papyrifera* was extracted in separate flasks (100 g of dry bark each) with 0.5 L of either chloroform, 50% ethanol, ethanol, methanol, or water, respectively, at room temperature for 5 days to examine the enzymatic inhibitory activities against glucosidase, mannosidase, and rhamnosidase as a function of solvent used (**Table1**). The chloroform extract was determined as target extract for the isolation of α-glucosidase inhibitors as it gave the strongest inhibition. The air-dried root bark (1.0 kg) of *B. papyrifera* was chopped and extracted with chloroform (10 L × 3) at room temperature for 5 days. The combined filtrate was concentrated in vacuo to yield a dark brown gum (87 g, 8.7%). This crude extract (30 g) was fractionated by silica gel flash CC employing a gradient of chloroform to acetone, resulting in five fractions (fractions A−E). To isolate the two new compounds **11** and **12**, fraction A (4.7 g) was fractionated by silica gel flash CC employing a gradient of hexane to EtOAc, resulting in 11 subfractions (A1−A11). Subfractions A8 and A9, enriched with **11** and **12**, were combined (460 mg) and further purified by silica gel flash CC to yield compounds **11** (25 mg, 0.007%) and **12** (15 mg, 0.004%).

The pure compounds **1**−**10** have been isolated by different chromatographic methods and characterized as described previously (*1*, *15*−*21*). Fraction B (5.2 g) was fractionated by silica gel flash CC employing a gradient of hexane to EtOAc resulting in nine subfractions (B1−B9). Subfractions B6−B8, enriched with **5**−**8**, were combined (870 mg) and further purified by silica gel flash CC to yield compounds **5** (52 mg, 0.015%) and **6** (65 mg, 0.018%) and a mixture of compounds **7** and **8**. Further purification by Sephadex LH-20 (Pharmacia Biotech AB, Uppsala, Sweden) with CH_3OH as eluent yielded compounds **7** (95 mg, 0.027%) and **8** (37 mg, 0.011%). Fraction D (8.8 g) was subjected to flash CC employing a gradient $CHCl_3$ to acetone, giving 12 subfractions (D1−D12). Subfractions D3 and D4, enriched with **1**−**4**, were combined (510 mg) and further purified by reversed-phase CC (ODS-A, 12 nm, S-150 μM) eluting with CH_3OH/H_2O (4:1) to afford compounds **1** (115 mg, 0.033%), **2** (66 mg, 0.019%), **3** (10 mg, 0.003%), and **4** (15 mg, 0.004%). Fraction D5 (163 mg) was subjected to flash CC employing $CHCl_3$/acetone gradient (30:1 → 5:1) to give compounds **9** (57 mg, 0.017%) and **10** (64 mg, 0.019%).

Broussochalcone A (***1***)*:* yellow needles; mp 182−184 °C; EIMS *m*/*z* 340 $[M]^+$; HREIMS, *m*/*z* 340.1313 (calcd for $C_{20}H_{20}O_5$, 340.1311); ^1H and ^{13}C NMR consistent with previously published data (*16*).

Broussochalcone B (***2***)*:* yellow needles; mp 168−169 °C; EIMS, *m*/*z* 324 $[M]^+$; HREIMS, *m*/*z* 324.1363 (calcd for $C_{20}H_{20}O_4$, 324.1362); ^1H and ^{13}C NMR consistent with previously published data (*16*).

3,4-Dihydroxyisolonchocarpin (***3***)*:* amorphous yellow powder; mp 242−243 °C; EIMS, *m*/*z* 338 $[M]^+$; HREIMS, *m*/*z* 338.1153 (calcd for $C_{20}H_{18}O_5$, 328.1154); ^1H and ^{13}C NMR consistent with previously published data (*20*).

4-Hydroxyisolonchocarpin (***4***)*:* amorphous yellow powder; mp 196−197 °C; EIMS, *m*/*z* 322 $[M]^+$; HREIMS, *m*/*z* 322.1203 (calcd for $C_{20}H_{20}O_4$, 322.1205); ^1H and ^{13}C NMR consistent with previously published data (*21*).

3′-(3-Methylbut-2-enyl)-3′,4′,7-trihydroxyflavane (***5***)*:* yellow sticky oil; $[\alpha]_D$ −5.8° ($CHCl_3$, *c* 0.35); EIMS, *m*/*z* 326 $[M]^+$; HREIMS, *m*/*z* 326.1516

Table 1. Comparison of Extraction Yield, α-Glucosidase, α-Mannosidase, and α-Rhamnosidase Inhibition of *B. papyrifera* Using Different Solvents[a]

		α-glucosidase		α-mannosidase		α-rhamnosidase	
extraction solvent	extraction yield[b] (%)	IC_{50} (μg/mL)	inhibition[c] (%)	IC_{50} (μg/mL)	inhibition[c] (%)	IC_{50} (μg/mL)	inhibition[c] (%)
chloroform	8.7 ± 2.2	9.3 ± 0.2	97.5 ± 5.3	198.5 ± 3.5	56.3 ± 2.6	nt[d]	12.2 ± 1.1
50% ethanol	14.4 ± 1.5	16.5 ± 0.3	96.3 ± 4.5	732.1 ± 2.3	17.2 ± 1.5	nt	3.5 ± 0.5
ethanol	12.6 ± 1.3	12.4 ± 0.6	91.7 ± 3.2	140.7 ± 1.8	91.1 ± 3.6	nt	8.3 ± 1.5
methanol	14.3 ± 1.0	11.5 ± 0.5	98.2 ± 2.2	175.5 ± 2.1	79.8 ± 1.8	nt	8.0 ± 0.8
water	10.9 ± 2.3	nd[e]	nd	nd	nd	nd	nd

[a] All extracts were examined in a set of experiments repeated three times. [b] Extraction yields are given as g/100 g of dry weight. [c] Sample concentration was 200 μg/mL. [d] nt, not tested. [e] nd, not detected.

Table 2. ^1H and ^{13}C NMR Data of New Compounds **11** and **12** in $CDCl_3$

	11			**12**		
position	δ_c	δ_H (mult, *J* in Hz)	HMBC	δ_c	δ_H (mult, *J* in Hz)	HMBC
2	150.0			150.3		
3	135.0			134.8		
4	171.0			170.9		
4a	106.9			106.9		
5	161.9			161.9		
6	102.1	6.28 (s)	C-4a,8	102.0	6.27 (s)	C-4a,8
7	161.4			161.3		
8	111.0			110.9		
8a	156.1			156.1		
1′	109.7			108.8		
2′	147.4			151.2		
3′	108.5			113.5		
4′	148.0			148.1		
5′	146.8			145.0		
6′	104.3	7.01 (s)	C-2,1′,4′,5′	98.2	6.90 (s)	C-2,1′,4′,5′
1″	41.9			41.9		
2″	28.5	1.68 (s)	C-8	28.3	1.75 (s)	C-8
3″	28.5	1.68 (s)	C-8	28.3	1.75 (s)	C-8
4″	149.6	6.43 (dd, 17.8, 10.4)		149.7	6.42 (dd, 17.8, 10.6)	
5″	113.7	5.32 (d, 10.4), 5.42 (d, 17.6)		113.5	5.42 (d, 17.5), 5.31 (d, 10.6)	
1‴	115.5	6.80 (d, 9.9)	C-2′,3′,4′	23.0	3.58 (d, 6.8)	C-2′,3′,4′
2‴	131.6	5.71 (d, 9.9)		119.2		
3‴	78.6			133.8		
4‴	18.7	1.48 (s)		26.1	1.70 (s)	
5‴	26.2	1.48 (s)		26.2	1.70 (s)	
1⁗	67.9	4.60 (d, 6.6)	C-5′	66.9	4.62 (d, 6.7)	C-5′
2⁗	120.6	5.44 (br t)		120.9	5.28 (br t)	
3⁗	138.3			140.0		
4⁗	28.7	1.72 (s)		18.3	1.77 (s)	
5⁗	28.7	1.72 (s)		18.7	1.83 (s)	
4-OH		12.9 (s)	C-4a,5,6		13.0 (s)	C-4a,5,6
7-OH		7.15	C-7,8			
4′-OH					6.32	C-3′,4′,5′

(calcd for $C_{20}H_{22}O_4$, 326.1518); ^1H and ^{13}C NMR consistent with previously published data (*5*).

Kazinol A (***6***)*:* yellowish powder; mp 129−130 °C; $[\alpha]_D$ −10.7° ($CHCl_3$, *c* 0.13); EIMS, *m*/*z* 394 $[M]^+$; HREIMS, *m*/*z* 394.2141 (calcd for $C_{25}H_{30}O_4$, 394.2144); ^1H and ^{13}C NMR consistent with previously published data (*15*).

Kazinol B (*7*)*:* amorphous yellow powder; mp 86−88 °C; $[\alpha]_D$ −19.0° ($CHCl_3$, *c* 0.38); EIMS, *m*/*z* 392 $[M]^+$; HREIMS, *m*/*z* 392.1989 (calcd for $C_{25}H_{28}O_4$, 392.1988); ^1H and ^{13}C NMR consistent with previously published data (*15*).

Kazinol E (***8***)*:* yellow sticky oil; $[\alpha]_D$ +0.33° ($CHCl_3$, *c* 0.41); EIMS, *m*/*z* 462 $[M]^+$; HREIMS, *m*/*z* 462.2761 (calcd for $C_{30}H_{38}O_4$, 462.2770); ^1H and ^{13}C NMR consistent with previously published data (*17*).

8-(1,1-Dimethylallyl)-5′-(3-methylbut-2-enyl)-3′,4′,5,7-tetrahydroxyflanvonol (***9***)*:* amorphous yellow powder; mp 73−74 °C; EIMS, *m*/*z* 438 $[M]^+$; HREIMS, *m*/*z* 438.1648 (calcd for $C_{25}H_{26}O_7$, 438.1679); ^1H and ^{13}C NMR consistent with previously published data (*5*).

Papyriflavonol A (***10***)*:* amorphous yellow powder; mp 202−204 °C; EIMS, *m*/*z* 438 $[M]^+$; HREIMS, *m*/*z* 438.1647 (calcd for $C_{25}H_{26}O_7$, 438.1679) ; ^1H and ^{13}C NMR consistent with previously published data (*1*).

Brossoflurenone A (***11***)*:* yellowish plate; mp 206−208 °C; IR, *ν* (KBr) cm^{-1} 2920, 1639, 1597, 1505, 1455; UV, λ_{max} nm 243, 292, 370 (CH_3CN); ^1H and ^{13}C NMR data, see **Table 1**; EIMS, *m*/*z* 502 $[M]^+$ (11), 487 (5), 434 (44), 419 (100), 389 (8), 377 (4), 335 (2), 281 (1); HREIMS, *m*/*z* 502.1995 (calcd for $C_{30}H_{30}O_7$, 502.1992); ^1H and ^{13}C NMR data, see **Table 2**.

Brossoflurenone B (***12***)*:* amorphous yellow powder; mp 186−187 °C; IR, *ν* (KBr) cm^{-1} 2921, 1649, 1506, 1455; UV, λ_{max} nm 269, 297, 357 (CH_3CN); ^1H and ^{13}C NMR data, see **Table 1**; EIMS, *m*/*z* 504 $[M]^+$ (22), 452 (1), 436 (100), 421 (94), 381 (45), 365 (31), 325 (15), 309 (4), 281 (3); HREIMS, *m*/*z* 504.2152 (calcd for $C_{30}H_{32}O_7$, 504.2148); ^1H and ^{13}C NMR data, see **Table 2**.

Enzyme Assay. *α-Glucosidase and α-L-Rhamnosidase Activity*. α-Glucosidase (EC 3.2.1.20) and α-L-rhamnosidase (EC 3.2.1.40) activities were assayed according to the methods described by Seo and Kim (*22*, *23*) with some minor modifications. The reaction mixture consisted of the enzyme solution (0.02 unit of α-glucosidase, 50 μL;

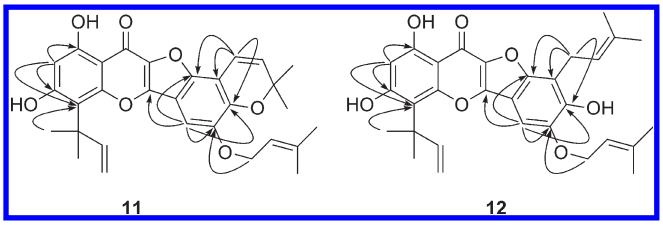

Figure 2. Important HMBC correlations of compounds **11** and **12**.

0.2 unit of α-L-rhamnosidase, 50 μL), substrate (1 mM *p*-nitrophenyl-α-D-glucopyranoside, 50 μL; 2.5 mM *p*-nitrophenol-α-D-rhamnopyranoside, 100 μL) in 50 mM potassium phosphate buffer (pH 6.8), and test sample in 5% DMSO (10 μL). After incubation for 30 min at 37 °C, the reaction was stopped by adding 2 M NaOH. The released *p*-nitrophenol was measured spectrometrically at 405 nm. The inhibitory effects of the tested compounds were expressed as the concentration that inhibits 50% of the enzyme activity (IC_{50}). Kinetic parameters were determined using the Lineweaver−Burk double-reciprocal plot method at increasing concentrations of substrates and inhibitors. The IC_{50} values were then calculated using SigmaPlot program (Systat Software Inc.).

α-Mannosidase Activity. α-Mannosidase (EC 3.2.1.24) activity was assayed according to the method described by Kato (*24*) with minor modifications. α-Mannosidase (0.1 U/mL) was dissolved in 50 mM sodium acetate buffer (pH 4.5) and used as an enzyme solution. Ten millimolar *p*-nitrophenyl-α-D-manopyranoside (100 μM) in the same buffer (50 mM sodium acetate, pH 4.5) was used as a substrate solution. The enzyme solution (25 μL) and test extracts (10 μL) dissolved in dimethyl sulfoxide at a concentration of 5% were mixed in a well of a microtiter plate and measured for titer (Abs 405 nm) at zero time using a microplate reader (expert 96, Asys). The increase in absorbance from zero time was measured. The inhibitory activity was expressed as 30 min relative absorbance difference (%) of test extract to absorbance change of the control, when test solution (extract in 10 μL dimethyl sulfoxide) was replaced by neat dimethyl sulfoxide. All determinations were performed in triplicate.

RESULTS AND DISCUSSION

The extracts from five different polar solvents were tested for their enzymatic inhibitory activities against α-glucosidase and α-mannosidase. The enzyme was assayed according to a standard literature procedure by following the hydrolysis of nitrophenyl glycoside spectrophotometrically (*22*−*24*). As shown in **Table 1**, all extracts investigated apart from the water extract exhibited a significant degree of α-glucosidase inhibition with IC_{50} of around 10 μg/mL and a moderate degree of α-mannosidase (IC_{50} > 150 μg/mL) inhibition. The high potency of the chloroform extract encouraged us to identify the compounds responsible for its α-glucosidase inhibitory effect.

Activity-guided fractionation of the chloroform extract gave 12 polyphenols **1**−**12**, which were purified over silica gel, Sephadex LH-20, and octadecyl-functionlized silica gel as delineated above. Isolated compounds (**1**−**10**) were identified as the known species broussochalcone A (**1**), broussochalcone B (**2**), 3,4-dihydroxyisolonchocarpin (**3**), 4-hydroxyisolonchocarpin (**4**), 3′-(3-methylbut-2-enyl)-3′,4′,7-trihydroxyflavane (**5**), kazinol A (**6**), kazinol B (**7**), kazinol E (**8**), 8-(1,1-dimethylallyl)-5′-(3-methylbut-2-enyl)-3′,4′,5,7-tetrahydroxyflavonol (**9**), and papyriflavonol A (**10**) through analysis of spectroscopic data and comparison with previous studies (*1*, *15*−*21*).

The remaining two compounds emerged to be hitherto uncharacterized, and their structural elucidation is now delineated. Compound **11** was obtained a yellowish paste having the molecular formula $C_{30}H_{30}O_7$ and 16 degrees of unsaturation established by HREIMS (*m*/*z* 502.1995 $[M]^+$). ^1H and ^{13}C NMR data in conjunction with DEPT experiments indicated the presence of 30 carbon atoms, consisting of the following functional groups:

Table 3. Inhibitory Effects of Compounds **1**−**12** on α-Glucosidase Activities

	α-glucosidase	
compound	IC_{50}[a] (μM)	type of inhibition K_i[b] (μM)
1	5.3 ± 0.3	noncompetitive (7.2 ± 1.1)
2	11.1 ± 0.5	noncompetitive (16.2 ± 0.3)
3	19.1 ± 1.0	noncompetitive (8.1 ± 0.2)
4	12.3 ± 0.1	noncompetitive (9.7 ± 1.3)
5	75.7 ± 2.0	mixed (46.2 ± 0.5)
6	12.0 ± 0.8	mixed (13.6 ± 0.3)
7	26.3 ± 2.3	mixed (20.3 ± 2.5)
8	10.6 ± 1.5	mixed (4.9 ± 0.1)
9	3.6 ± 0.4	mixed (4.2 ± 0.4)
10	2.1 ± 0.2	mixed (2.3 ± 0.3)
11	27.6 ± 1.3	mixed (12.1 ± 1.2)
12	33.3 ± 0.0.4	mixed (13.6 ± 1.0)

[a] All compounds were examined in a set of experiments repeated three times; IC_{50} values of compounds represent the concentration that caused 50% enzyme activity loss. [b] Values of inhibition constant.

1 methylene (sp^2), 6 methines (sp^2), 6 methyls (sp^3), and 16 quaternary carbons. The ^{13}C NMR data enabled carbons corresponding to the 10 C−C double bonds and 1 carbonyl group to be identified and, thus, accounted for 11 of 16 degrees of unsaturation. The extra five degrees of unsaturation were ascribed to five rings, two of which were aromatic. The presence of a 1,1-dimethylallyl group was easily deduced from successive connectivity between H-5″ (δ_H 5.32 and 5.42) and H-4″ (δ_H 6.43) in the COSY spectral data and HMBC correlation of H-4″ with C-1″ (δ_C 41.9) and C-2″ (δ_C 28.5). HMBC correlation of the peak at δ_H 1.68 (H-2″ and H-3″) with C-8 (δ_C 111.0) unveiled the location of the 1,1-dimethylallyl moiety. The presence of a 3,3-dimethylallyloxy group was deduced from the successive connectivity from methylene proton H-1‴″ (δ_H 4.60) to methyl proton (δ_H 1.72) in the COSY spectrum. A strong HMBC correlation between H-1‴″ (δ_H 4.60) and C-5′ (δ_C 146.8) proved the location of the 3,3-dimethylallyloxy group. Moreover, in the mass spectrum of **11**, loss of a 3,3-dimethylallyl group from the molecular ion gave a strong peak at *m*/*z* 434, consistent with our proposed structure. The connectivity between H-1‴ (δ_H 6.80) and H-2‴ (δ_H 5.71) in COSY spectral data and HMBC correlation of H-4‴ (δ_H 1.48) with C-3‴ (δ_C 78.6) and C-2‴ (δ_C 120.6) indicated the presence of a 2,2-dimethylchromeno ring. The position of the substituent on the ring system was determined by the HMBC correlations of H-1‴ with C-3′ (δ_C 108.5), C-4′ (δ_C 148.0), and C-2′ (δ_C 147.4). The rare skeleton 5,11-dioxabenzo[*b*]fluoren-10-one was confirmed by HMBC correlation (**Figure 2**) of H-6′ (δ_H 7.01) with C-2 (δ_C 150.0) and C-2′ (δ_C 147.4) and chemical shift value. According to the previous report of a 10,11-dioxabenzo[*b*]fluoren-5-one ring system, C-3 appeared at a lower field (δ_C 164−165 ppm) and C-2 appeared at a much higher field (δ_C 112−115 ppm) in comparison with corresponding carbon positions (C-2 and C-3) of compound **11** (*25*). The 5,7-dihydroxybenzene moiety was easily confirmed by the presence of a hydrogen-bonded hydroxyl group (δ_H 12.90) and HMBC correlations of H-6 (δ_H 6.28) with both C-7 (δ_C 161.3) and C-4a (δ_C 161.9). Thus, compound **11** was identified as 3′,4′-(2,2-dimethylchromeno)-5′-(3,3-dimethylallyloxy)-5,7-dihydroxy-8-(1,1dimethylallyl)furano-[3,2-*b*]-4*H*-chromen-4-one and called brossoflurenone A.

Compound **12** was assigned the molecular formula $C_{30}H_{32}O_7$ (15 degrees of unsaturation) by analysis of its HREIMS (*m*/*z*, 504.2152 $[M]^+$). The ^1H, ^{13}C, and 2D NMR spectroscopic data for **12** revealed the presence of the same two side chains as those attached to C-5′ and C-8 in **11**. The only structural difference was observed in the isoprenyl group at C-3′. This group had undergone

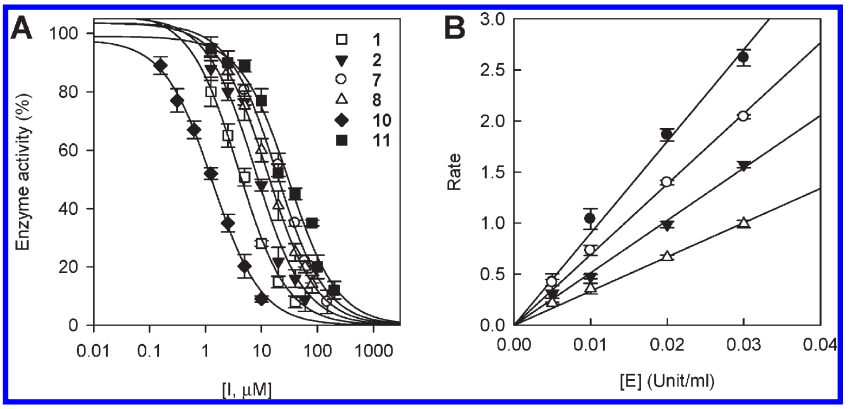

Figure 3. (**A**) Effect of compounds **1** (□), **2** (▼), **7** (○) **8** (△), **10** (◆), and **11** (■) on the activity of α-glucosidase for the hydrolysis of *p*-nitrophenyl-α-D-glucopyranoside. (**B**) Catalytic activity of α-glucosidase as a function of enzyme concentration at different concentrations of compound **10** (●, 0 μM; ○, 5 μM; ▼, 10 μM; □, 20 μM).

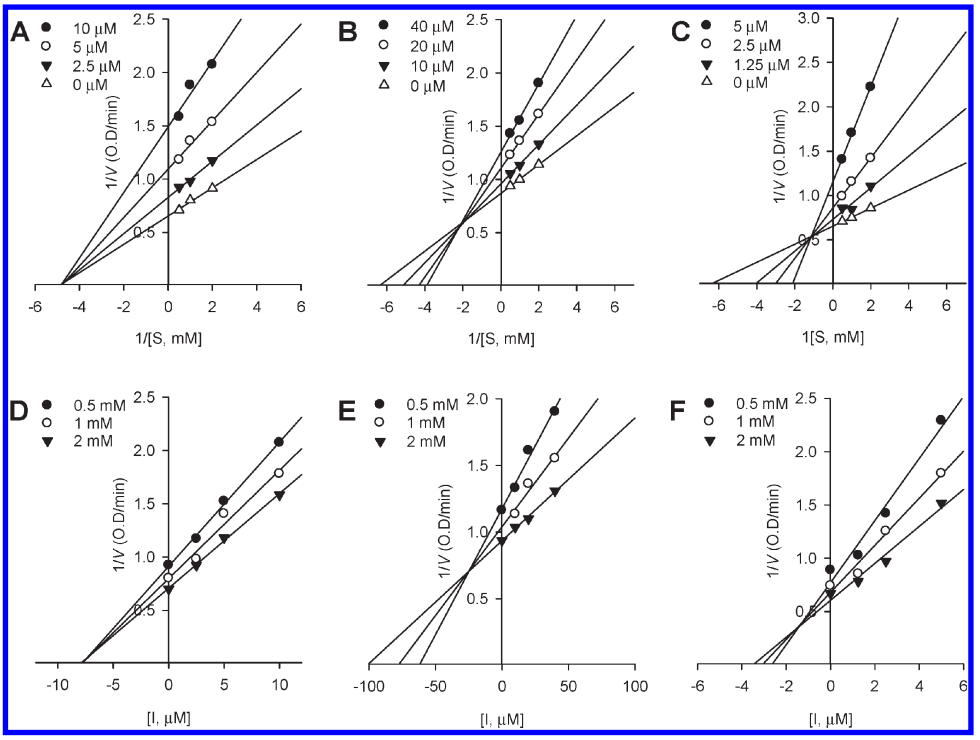

Figure 4. Graphical determination of the type of inhibition for compounds **1**, **7**, and **10**. **A**, **B**, and **C** are Lineweaver−Burk plots for the inhibition of compounds **1**, **7**, and **10** on the hydrolysis activity of α-glucosidase. Conditions were as follows: 1 mM *p*-nitrophenyl-α-D-glucopyranoside, 0.02 unit of α-glucosidase, and 50 mM potassium phosphate buffer (pH 6.8), at 37 °C, in the presence of different concentrations of compounds for lines, from bottom to top, (**A**) for compound **1** of 0, 2.5, 5, and 10 μM; (**B**) for compound **7** of 0, 10, 20, and 40 μM; and (**C**) for compound **10** of 0, 1.25, 2.5, and 5 μM. **D**, **E**, and **F** are Dixon plots for the inhibition of compounds **1**, **7**, and **10**, respectively, on the hydrolysis activity of α-glucosidase in the presence of different concentrations of substrate for lines, from bottom to top, of 2, 1, and 0.5 mM.

an oxidative cyclization with its adjacent hydroxyl group on C-4′ to form a 2,2-dimethylpyran ring in compound **11**. The second isoprenyl group [at C(1)] remains uncyclized. The cyclized isoprenyl group at C(1) was confirmed by successive connectivity from H-1‴ (δ_H 3.58) to H-5‴ (δ_H 1.70) in the COSY spectrum. The strong HMBC correlation of H-1‴ with C-3′ (δ_C 113.5), C-4′ (δ_C 148.1), and C-2′ (δ_C 151.2) proved the location of an isoprenyl group on C-3′. The key core, 5,11-dioxabenzo[*b*]fluoren-10-one, was confirmed with the HMBC correlations starting from H-6′ and chemical shifts of C-2 (δ_C 150.3) and C-3 (δ_C 134.8), which showed a pattern very similar to that of compound **11** (**Figure 2**). Thus, compound **12** was identified as 3′-(2,2-dimethylallyl)-5′-(3,3-dimethylallyloxy)-4′,5,7-trihydroxy-8-(1,1-dimethylallyl)-furano[3,2-*b*]-4*H*-chromen-4-one and called brossoflurenone B.

The inhibitory potencies and capacities of these polyphenols toward α-glucosidase were investigated. The inhibitory profiles of compounds **1**−**12** against α-glucosidase are shown in **Table 3**. All compounds showed a dose-dependent inhibitory effect on α-glucosdiase activity (**Figure 3A**). All chalcones (**1**−**4**) exhibited a significant degree of inhibition (IC_{50} = 5.3−19.1 μM). However, the activity was slightly affected by subtle changes in structure. The prenylated chalcone (**1**) with a catechol moiety in the B ring and a resorcinol moiety in the A ring was the most effective chalcone-derived inhibitor with an IC_{50} of 5.3 μM. Our results indicate that a free resorcinol motif within the A ring (**1** and **2**) was marginally preferred over the corresponding products of oxidative cyclization of the alcohol group onto the pendant allyl group (**3** and **4**). In the case of flavans (**5**−**8**),

4′,5′-diprenyl derivative **8** displayed the most potent inhibitory activity (IC_{50} = 10.6 μM). In a similar vein, the 2′,4′-diprenyl derivative **6** (IC_{50} = 12.0 μM) was of similar potency. On the other hand, compound **5**, bearing only one prenyl group on the C ring, exhibited the lowest activity (IC_{50} = 75.7 μM). Taken together, it seems that an increasing number of prenyl groups increases the potency of the inhibitor. Similar trends can also be seen in flavanols (**9** and **10**) and dioxabenzo[*b*]fluoren-10-one, which showed respectively similar inhibitory activities as they had similar levels of prenylation. Interestingly, the efficacy of the inhibitors appears to be relatively insensitive to steric effects α to the phenyl ring (for instance, **9**, bearing a quaternary center at C-8, and **10**, bearing an allyl group at C-6 had IC_{50} values differing by a factor of <2). Pleasingly, the potency of the most effective inhibitor **10** (IC_{50} = 2.1 μM) compares favorably with one of the most potent α-glucosidase inhibitors known, deoxynojirimycin (IC_{50} = 3.5 μM) (*26*). The novel α-glucosidase inhibitors **11** (IC_{50} = 27.6 μM) and **12** (IC_{50} = 33.3 μM) are similar in potency to sugar-derived α-glucosidase inhibitors, such as voglibose (IC_{50} = 23.4 μM), which is currently used for therapeutic purposes (*27*).

Kinetic analysis of the inhibitors, as depicted in **Figure 4**, elucidated typical progress curves for reversible, noncompetitive, or mixed-type inhibitors. All of the compounds manifested the same relationship between enzyme activity and enzyme concentration. The inhibition of α-glucosidase by compound **10** (the most effective species) is illustrated in **Figure 3B**, representatively. Plots of the initial velocity versus enzyme concentrations in the presence of different concentrations of compound **10** gave a family of straight lines, all of which passed through the origin. Increasing the inhibitor concentration resulted in lowering of the slope of the line, indicating that these compounds were reversible inhibitors. The enzyme inhibition properties of these derivatives were modeled using double-reciprocal plots (Lineweaver−Burk and Dixon analyses). This analysis (**Figure 4A**) showed that V_{max} decreased without changing K_m in the presence of increasing concentrations of inhibitors: as can be seen directly from the graph, $-1/K_m$ (the *x*-intercept) was unaffected by inhibitor concentration, whereas $1/V_{max}$ became more positive. This behavior indicates that prenyl chalcones (**1**−**4**) exhibit noncompetitive inhibition characteristics for α-glucosidase. The K_i value of these chalcones was easily measured from **Figure 4D**. On the other hand, the flavan (**5**−**8**) and flavonol (**9**−**12**) series displayed a different inhibition profile for α-glucosidase. A similar analysis of these compounds shows a series of lines, which intersect to the left of the vertical axis and above the horizontal axis (**Figure 4B**,**C**), indicating that these inhibitors were mixed-type inhibitors. The mixed-type behavior of compounds (**5**−**12**) was also shown by Dixon plots in Figure **4E**,**F**.

In conclusion, we have undertaken a thorough investigation into the α-glucosidase inhibition of extracts from the important medicinal plant *B. papyrifera*. The principal components were typical of cellular extracts from this species, chalcones, flavans, and flavonols; however, we were able to extract two novel compounds, both of which we showed to have the unusual 5,11-dioxabenzo[*b*]fluoren-10-one motif. In this way we have found the first examples of α-glucosidase inhibitors from this important plant. Furthermore, we have uncovered some of the most potent inhibitors of α-glucosidase known (lowest IC_{50} = 2.1 μM). Our SAR uncovered some interesting aspects of these species, including the requirement for hydrophobic groups around the aromatic core and an indifference to steric bulk around the ring. Given the huge importance of α-glucosidase inhibitors in medicinal chemistry, we believe that these lead compounds could be of great significance to research in this pervasive field.

ABBREVIATIONS USED

IC_{50}, inhibitor concentration leading to 50% activity loss; K_i, inhibition constant; K_m, Michaelis constant; PTP1B, protein tyrosine phosphatase 1B; SAR, structure−activity relationship.

Supporting Information Available: Characterization data and kinetic plots. This material is available free of charge via the Internet at http://pubs.acs.org.

LITERATURE CITED

(1) Zhang, P. C.; Wang, S.; Wu, Y.; Chen, R. Y.; Yu, D. Q. Five new diprenylated flavonols from the leaves of *Broussonetia kazinoki*. *J. Nat. Prod.* **2001**, *64*, 1206–1209.

(2) Takasugi, M.; Niino, N.; Nagao, S.; Anetai, M.; Masamune, T.; Shirata, A.; Takahashi, K. Eight minor phytoalexins from diseased paper mulberry. *Chem. Lett.* **1984**, 689–692.

(3) Wang, J. P.; Tsao, L. T.; Raung, S. L.; Lin, C. N. The signal transduction mechanism involved in kazinol B-stimulated superoxide anion generation in rat neutrophils. *Br. J. Pharmacol.* **1998**, *125*, 517–525.

(4) Chen, Z. J.; Lin, C. N.; Hwang, T. L.; Teng, C. M. Broussochalcone A, a potent antioxidant and effective suppressor of inducible nitric oxide synthase in lipopolysaccharide-activated macrophages. *Biochem. Pharmacol.* **2001**, *61*, 939–946.

(5) Chen, R. M.; Hu, L. H.; An, T. Y.; Li, J.; Shen, Q. Natural PTP1B inhibitors from *Broussonetia papyrifera*. *Bioorg. Med. Chem. Lett.* **2002**, *12*, 3387–3390.

(6) Zheng, Z. P.; Cheng, K. W.; Chao, J.; Wu, J.; Wang, M. Tyrosinase inhibitors from paper mulberry (*Boussonetia papyrifera*). *Food Chem.* **2008**, *106*, 529–535.

(7) Floris, A. L.; Peter, L. L.; Reinier, P. A.; Eloy, H. L.; Guy, E. R.; Chris, W. α-Glucosidase inhibitors for patients with type 2 diabetes: results from a cochrane systematic review and meta-analysis. *Diabetes Care* **2005**, *28*, 154–163.

(8) Fernandes, B.; Sagman, U.; Auger, M.; Demetrio, M.; Dennis, J. W. β1−6 branched oligosaccharides as a marker of tumor progression in human breast and colon neoplasia. *Cancer Res.* **1991**, *51*, 718–723.

(9) Seiichiro, O.; Ayako, M.; Takashi, O.; Hideya, Y.; Hironobu, H. Synthesis and biological evaluation of α-L-fucosidase inhibitors: 5a-carba-α-L-fucopyranosylamine and related compounds. *Eur. J. Org. Chem.* **2001**, *5*, 967–974.

(10) Ernst, H. A.; Leggio, L. L.; Willemoes, M.; Leonard, G.; Blum, P.; Larsen, S. Structure of the *Sulfolobus solfataricus* alpha-glucosidase: implications for domain conservation and substrate recognition in GH31. *J. Mol. Biol.* **2006**, *358*, 1106–1124.

(11) Ellgaard, L.; Helenius, A. Quality control in the endoplasmic reticulum. *Nat. Rev. Mol. Cell Biol.* **2003**, *4*, 181–191.

(12) Asano, N. Glycosidase inhibitors: update and perspectives on practical use. *Glycobiology* **2003**, *13*, 93R–104R.

(13) Dwek, R. A.; Butters, T. D.; Platt, F. M.; Zitzmann, N. Targeting glycosylation as a therapeutic approach. *Nat. Rev. Drug Discov.* **2002**, *1*, 65–75.

(14) Jacob, G. S. Glycosylation inhibitors in biology and medicine. *Curr. Opin. Struct. Biol.* **1995**, *5*, 605–611.

(15) Ikut, J.; Hano, Y.; Nomura, T. Compounds of *Broussonetia papyrifera* (L.) Vent. 2. Structure of two new isoprenylated flavans, kazinols A and B. *Heterocycles* **1985**, *23*, 2835–2842.

(16) Matsumoto, J.; Fujimoto, T.; Takino, C.; Saitoh, M.; Hano, Y.; Fukai, T.; Nomura, T. Components of *Broussonetia papyrifera* (L.) Vent. I. Structures of two new isoprenylated flavonols and two chalcone derivatives. *Chem. Pharm. Bull.* **1985**, *33*, 3250–3256.

(17) Ikauta, J.; Hano, Y.; Nomura, T.; Kawakami, Y.; Sato, T. Components of *Broussonetia kazinoki* SIEB. I. Structure of two new isoprenylated flavans and five new isoprenylated 1,3-diphenylpropane derivatives. *Chem. Pharm. Bull.* **1986**, *34*, 1968–1979.

(18) Lee, D. H.; Bhat, K. P. L.; Fong, H. H. S.; Farnsworth, N. R.; Pezzuto, J. M.; Kinghorn, A. D. Aromatase inhibitors from *Broussonetia papyrifera*. *J. Nat. Prod.* **2001**, *64*, 1286–1293.
(19) Ko, H. H.; Yu, S. M.; Ko, F. N.; Teng, C. M.; Lin, C. N. Bioactive constituents of *Morus australis* and *Broussonetia papyrifera*. *J. Nat. Prod.* **1997**, *60*, 1008–1011.
(20) Filho, R. B.; Gottiieb, O. R.; Mourao, A. P.; Rocha, A. I. D.; Oliveira, F. S. Flovonoids from *Derris* species. *Phytochemistry* **1975**, *14*, 1454–1456.
(21) Dagne, E.; Bekele, A.; Waterman, P. G. The flavonoids of *Millettia ferruginea* subsp. *ferruginea* and subsp. *darassana* in Ethiopia. *Phytochemistry* **1989**, *28*, 1897–1900.
(22) Seo, E. J.; Marcus, J. C. L.; Lee, B. W.; Kim, H. Y.; Ryu, Y. B.; Jeong, T. S.; Lee, W. S.; Park, K. H. Xanthones from *Cudrania tricuspidata* displaying potent α-glucosidase inhibition. *Bioorg. Med. Chem. Lett.* **2007**, *17*, 6421–6424.
(23) Kim, J. H.; Marcus, J. C. L.; Seo, W. D.; Lee, J. H.; Lee, B. W.; Yoon, Y. J.; Kang, K. Y.; Park, K. H. α-Rhamnosidase inhibitory activities of polyhydroxylated pyrrolidine. *Bioorg. Med. Chem. Lett.* **2005**, *15*, 4282–4285.
(24) Kato, A.; Kato, N.; Kano, E.; Adachi, I.; Ikeda, K.; Yu, L.; Okamoto, T.; Banba, Y.; Ouchi, H.; Takahata, H.; Asano, N. Biological properties of D- and L-1-deoxyazasugars. *J. Med. Chem.* **2005**, *48*, 2036–2044.
(25) Xiang, W.; Li, R. T.; Mao, Y. L.; Zhang, H. J.; Li, S. H.; Song, Q. S.; Sun, H. D. Four new prenylated isoflavonoids in *Tadehagi triquetrum*. *J. Agric. Food Chem.* **2005**, *53*, 267–271.
(26) Romaniouk, A. V.; Silva, A.; Feng, J.; Vijay, I. K. Synthesis of a novel photoaffinity derivative of 1-deoxynojirimycin for active site-directed labeling of glucosidase I. *Glycobiology* **2004**, *14*, 301–310.
(27) Adisakwattana, S.; Ngamrojanavanich, N.; Kalampakorn, K.; Tiravanit, W.; Roengsumran, S.; Yibchok-Anun, S. Inhibitory activity of cyaniding-3-rutinoside on α-glucosidase. *J. Enzyme Inhib. Med. Chem* **2004**, *19*, 313–316.

Received for review September 1, 2009. Revised manuscript received November 10, 2009. Accepted November 14, 2009. This work was supported by the Korea Science and Engineering Foundation (KOSEF) grant funded by the Korean government (MEST) (No. 20090081751). H.W.R. was supported by a scholarship from the BK21 program.